Research Article

Open Access

Journal of Chemical Reactions and Catalysis Research

jcrc@scientificeminencegroup.com

Highly compacted and stable CdSe/TiO_2 electrodeposited heterostructure for improving simultaneous photoelectrochemical and photocatalytic performances

JOUDI Fedia, DRIDI Donia*, LITAIEM Yousra, BEN NACEUR Jamila, DIMASSI Wissem and CHTOUROU Radhouane

Laboratory of Nanomaterials and Systems for Renewable Energies (LaNSER), Research and Technology Center of Energy, Technopôle Borj-Cedria, Hammam-Lif, Tunis, Tunisia

*** Corresponding Author**

Dridi Donia, Laboratory of Nanomaterials and Systems for Renewable Energies (LaNSER), Research and Technology Center of Energy, Technopôle Borj-Cedria, Hammam-Lif, Tunis, Tunisia, Tel: +216) 29 483 509, Email: donia.dridi88@gmail.com

Citation

JOUDI Fedia, DRIDI Donia, LITAIEM Yousra, BEN NACEUR Jamila, DIMASSI Wissem and CHTOUROU Radhouane (2022) Highly and Stable CdSe/TiO2 Electrodeposited Heterostructure for Improving Simultaneous Photoelectrochemical and Photocatalytic Performances. J Chem Reac Catal Res 1: 1-18

Publication Dates

Received date: May 25, 2022
Accepted date: July 19, 2022
Published date: July 21, 2022

Abstract

In this work, highly compacted and stable Cadmium Selenide/Titanium Dioxide (CdSe/TiO_2) heterostructure has been designed through a low cost and easy electrochemical deposition strategy for improving simultaneous photoelectrochemical and photocatalytic performances. At one step, TiO_2 layers were deposited onto indium doped tin oxide (ITO) conductive glass substrates by sol-gel via spin-coating method. At a second step, the prepared TiO_2/ITO sample was used as working electrode for the CdSe electrodeposition approach from ionic liquid/organic solvent (tri-noctylmethyl-ammonium chloride (TOMAC))/Formamide (FA) based electrolyte. Structural, morphological, optical, photoelectrocemical (PEC) and photocatalytic properties of bare TiO_2 and CdSe/TiO_2 photoanodes (PAs) have been studied. Raman analysis confirms the obtained X-Ray Diffraction results by exhibiting the characteristic peaks for the anatase type and hexagonal phase of TiO_2. Morphological investigation by Atomic force microscopy (AFM) shows a dense, homogeneous and a surface covered with well distributed small spherical shaped grains for bare TiO_2 layer. Its root mean square (RMS) surface roughness has rised from 1.08 nm to 38.833 nm after electrodeposition of CdSe. In order to confirm these AFM results, scanning electron microscopy investigation reveals a surface clearly filled with granular shapes for bare TiO_2 layer. Then, the morphology has been modified and consisting of well distributed and agglomerated small grains on the surface of TiO_2 resulted from the growth of CdSe film. As compared to bare TiO_2, optical measurements show better charge

separation efficiency for the CdSe/TiO_2 heterostructure. The electrodeposition of highly compacted CdSe onto TiO_2/ITO has resulted in enhanced photocurrent density of 0.30 mA/cm^2 at 0.5V which is 7.5 times higher than bare TiO_2 when exposed to visible light irradiation. The sensitization process of TiO_2 with CdSe has also improved photocatalytic degradation efficiency of TiO_2 towards Methlylen Blue and Methyl Orange pollutant dyes thanks to the enhancement of its absorption capacity and charge separation rate of photogenerated carriers. The sensitization of TiO_2 with CdSe has resulted in a low cost and high stable CdSe/TiO_2 promising photoanodes for both of PEC based solar cells and photocatalytic degradation applications and consequently ccould overcome the serious environmental issues.

Keywords: CdSe/TiO_2, Electrodeposition, Sensitization, Electrolyte, Photoelectrochemical performance, Photocatalytic Degradation

Introduction

Thanks to Fujishima and Honda discovery related to the solar driven photocatalytic splitting of water on TiO_2 photoelectrodes in the early 1970s [1], photocatalytic and photoelectrochemical processes have been widely emerged as low cost and efficient environmental key solutions to tackle serious energy crisis and worldwide pollution issues [2,3]. Despite the outstanding features of TiO_2 including its eco-friendliness, cost-effectiveness, robustness, corrosion stability, high electrical and optical properties and strong photocatalytic activity [4,5], its wide band gap of 3.0eV for rutile and 3.2eV for anatase has severely affected its photoresponse which get limited to only 5% in the ultraviolet region of sunlight energy and resulted in lower photoconversion efficiency due to the high recombination rates of photogenerated eloctron-hole pairs [6]. In order to adress that issue, several strategies have been investigated to extend the light response field of TiO_2 to visible light and minimizing the recombination rates of the photoexcited charge carriers through doping [7-10], surface modification [11,12] and coupling TiO_2 with narrow band-gap semiconductors [13-15]. In particular, nanostructured II–VI semiconductors based on cadmium chalogenides are globally used as light harvesters such as cadmium telluride and cadmium selenide thanks to its high values of absorption coefficient. Precisely, Cadmium Selenide, named also cadmoselite (CdSe) earned recognizable interest as noteworthy active material to alter TiO_2 thanks to its exclusive and special properties namely its reduced band gap (1.7 eV) near to visible spectrum, high absorption coefficient, n-type conductivity, low resistivity, luminescent properties and its direct and reduced band gap around 1.73 eV which is characteristic of the solar spectrum radiation [16]. To date, huge research efforts have been conducted on seeking for the best and low cost technology to sensitize TiO_2 with CdSe for improving photoelectrochemical performance. By doing a literature survey, several research groups have extensively proposed either chemical bath deposition strategy [17-26] or SILAR approach [26-30] for the CdSe sensitization of TiO_2 and reported its effect on photoelectrochemical performance (Table1). However, these two direct deposition techniques have restricted application in coating onto substrates and consume long deposition time. Thereby, it is necessary to establish a low cost and simple strategy for the design of highly efficient CdSe/TiO_2 photoanodes. Interestingly, electrodeposition method has owned huge interest in recent years since it has numerous advantages including its low cost of synthesis, its environmentally friendly, its simple operating conditions, efficiently adjustability of different parameters like temperature, chemical composition, morphology, area and thichness, last but not least it produces CdSe films at a very high yield.

Table 1: Photoelectrochemical performance summary of $CdSe/TiO_2$ based photoanodes synthesized with CBD and Silar strategies between 2010-2020

Photosensitization approach	J_{sc} [mA/cm²]]	V_{oc}	FF	η [%]	Ref
CBD	1.7	-	-	-	[17]
CBD	12.6	0.74	44	4.14	[18]
CBD	11.33	0.395	42.8	3.83	[19]
CBD	10.9	0.395	49.4	2.13	[20]
CBD	12.1	0.45	32.1	1.75	[21]
CBD	6.2	0.54	53	1.8	[22]
CBD	9.74	0.49	34	1.6	[23]
CBD/Silar	13.6	0.57	52	3.95	[26]
Silar	4.68	0.43	24.2	0.48	[27]
Silar	8.16	0.58	41	2.15	[28]
Silar	9.72	0.492	47	2.26	[29]
Silar	10.32	0.517	49	2.65	[30]

Thus far, plenty of research groups have investigated the impact of various deposition parameters during the electrolysis process on the possibility to achieve enhanced photoelectrochemical performance of high controlled electrodeposited $CdSe/TiO_2$ photoanodes such as the deposition time, electrolyte's pH, type of electrolyte and the annealing treatment temperature (Table 2). In fact, Wang et al 2015 [31] reported potentiostatically electrodeposition of CdSe onto anodized TiO2 nanotube arrays. (NTAs) at various deposition time (30s, 35, 25s, 20s and 60s). They concluded that the deposition time of 30 s displayed excellent PEC performance by exhibiting a maximum photocurrent intensity of ~1 mA/cm² versus saturated calomel electrode (SCE) under visible light irradiation at 0.5 V. They ascribed this result to the high dispersity of CdSe nanoparticles on both inside and outside of the TiO_2 NTAs pore walls, the strong combination and heterojunctions between CdSe and TiO_2 through Cd-O bonds. In 2018, Ayal's research group [32] have synthesized CdSe / TiO_2 heterostructure through pulse electrodeposition method and studied the effect of different duty cycles varying from 10 % to 90 % on photoelectrochemical properties. They found that duty cycles played a crucial role in the formation of CdSe nanoparticles. The maximum photocurrent was evaluated to be 1.94 mA/cm² vs Ag/AgCl which has been obtained at a duty cycle of 50 %. The reached photoconversion efficiency was 1.18% which is 59 times higher than nude TiO_2. In 2013, Xue and co-workers [33] have prepared photoabsorbing CdSe electrodeposited films onto anodized TiO_2 from an acidic bath and studied the effect of the SeO_2 concentration (0, 2, 4, 6, 8 and 10 mM). on the PEC performance. At a precise SeO_2 content of 4 mM shows a maximum photocurrent of 7.72 mA/cm² vs SCE under visible light irradiation with a V_{oc} value of 1.24 V and an optimum efficiency of 7.1 %. In 2016, the same group of Ayal [34] have potentiostatically electrodeposited CdSe layer onto TiO_2 films and reported the effect of various pH values (1.0, 2.0, 3.0 and 3.3) on its PEC performance. The maximum photocurrent density of 2.13 mA/cm² vs Ag/AgCl under halogen light irradiation was reported at a pH of 3. The highest photoconversion efficiency was 1.02 % which is 51 times higher than bare TiO_2 nanotube array. This enhanced photoresponse may be due to the formation of well crystallized CdSe nanocrystals which were well bonded with TiO_2. In 2014, Xue and his colleagues [35] have investigated the impact of electrolyte's pH on PEC performance of electrodeposited CdSe on TiO_2 layers. They have varied the pH values from 1 to 4 and they found that pH value of 3 has exhibited the maximum photocurrent density around 4.0 mA/cm² at 0.5 V (vs SCE) which is 7 times higher than bare TiO_2 NTAs and a V_{oc} of -1.26 V. In 2017, Ayal's team work [36] have investigated the effect of thermal annealing on the enhancement of PEC properties of electrodeposited CdSe onto anodized TiO_2. They deduced that annealing treatment play an important role in controlling the formation of CdSe nanoparticles on TiO_2. The highest photocurrent density and photoconversion efficiency achieved values were 2.98 mA/cm² vs Ag/AgCl and 1.67 % respectively obtained at an annealing temperature of 250 °C

Table 2: Summary of synthesis conditions and PEC performance of electro deposited CdSe onto TiO_2 films for water splitting reported in 2013-2019

Electrodeposition Conditions	Electrolyte	PEC measurements	Ref
potentiostatic electrodeposition; Eapp = -0.9 V deposition time = 30 s, 35, 25 s, 20 s and 60 s at room temperature.	Aqueous solution; [$CdCl_2$]= 0.2 M 12.6 g Na_2SO_3, 3.2 g Se powder and 200 mL purified water	At t_{dep}= 30 s, $J_{sc,\ max}$ = ~ 1mA/cm^2 at 0.5 V vs SCE under visible light irradiation 300 W Xe lamp with an UV filter (> 400 nm)	[31]
Pulse electrodeposition; applying square pulse potential of -0.85 V as on-potential and 0.00 V as off-potential voltages duty cycles varying from 10 %, 25 %, 50 %, 75 % and 90 %	aqueous solution; [$CdCl_2$]=20 mM, [SeO_2]=5 mM and [Na_2SO_4]=20 mM (supporting electrolyte) in 100 mL of DI water.	At 50 % duty Cycle, $J_{sc,\ max}$ = 1.94 mA/cm^2 vs Ag/AgCl under illumination of halogen light and the reached photoconversion efficiency η of 1.18 %	[32]
2 cyclic voltammetry cycles. E_{app}= -0.4 V and -1.0 V (vs. SCE) pH = 3	Aqueous solution; [$CdCl_2{\cdot}5H_2O$]=0.1M [$C_4O_6H_4KNa$]=0.01M [SeO_2] = 0, 2, 4, 6, 8, 10 Mm in100 ml of DI water	At [SeO_2]= 4 mM SeO_2, $J_{sc\ max}$= 7.72 mA/cm^2 vs SCE, $V_{oc,\ max}$= 1.24 V and η_{max} = 7.1 % under 100 mW/cm^2 white light intensity from 500 W xenon lamp with 420 nm filter	[33]
potentiostatic electrodeposition; E_{app} = -0.7 V t_{dep} = 1800 s pH =1.0, 2.0, 3.0 and 3.3	Aqueous bath; [SeO_2] = 5 mM, [$CdCl_2{\cdot}5H_2O$]=0.02 M [Na_2SO_4]=0.02 M in 100 mL of DI water	At pH 3.0, $J_{sc\ max}$= 2.13 mA/cm^2 vs Ag/AgCl; $V_{oc,\ max}$ =-1.05 V under halogen light irradiation (300 W) and photoconversion efficiency of 1.02 %.	[34]
Cyclic voltammetry with 2 cycles E_{app} in the range of -0.4 V and -1.0 V. pH = 1, 2, 3 and 4	Aqueous bath; [$CdCl_2{\cdot}5H_2O$]=0.1 M[$C_4O_6H_4KNa$]=0.0 M [SeO_2] = 4 mM in 100 mL of DI water .	At pH = 3, $J_{sc,\ max}$ = 4.0 mA/cm^2 at 0.5 V(vs SCE), 7 times higher than bare TiO_2 NTAs Voc, max= -1.26 V under visible light from 500W Xenon lamp with 420 nm filter	[35]
potentiostatic electrodeposition; E_{app} of -0.7 V. Deposition time =30 min pH = 3.0	Aqueous bath; [$CdCl_2$]= 20 mM, [SeO_2] = 5 mM, [Na_2SO_4]= 20 mM As supporting electrolyte.	Upon annealing treatment temperature = 250 °C , $J_{sc,max}$ =2.98 mA/cm^2 vs Ag/AgCl and 1.67 % under solar illumination from a 300 W halogen lamp	[36]
IApp = −0.3 mA/cm^2 t_{dep}= 300 s, 400 s,500 s ,600 s and 700 s	Organic bath; [Se] = 5 Mm [$CdCl_2$]= 10 mM 30 mL of DMF heating at 125 °C in an oil bath	At t_{dep}=500 s, $J_{sc,max}$= 2.1 mA/cm^2 at 0 V (vs Ag/AgCl) under visible light irradiation ($\lambda \geq 420$ nm)	[37]

In 2019, Zhuang et al [37] were the first to publish the electrodeposition of CdSe photosensitizers onto TiO_2 films from an organic bath of N,N-dimethylformamide (DMF) and studying the effect of deposition time on the PEC properties of elaborated CdSe/TiO_2 photoanodes. At a deposition time of 500 s, enhanced photoelectrochemical (PEC) performance was achieved with a significant saturated photocurrent density of 2.1 mA/cm^2 at 0 V (vs Ag/AgCl) under visible light irradiation ($\lambda \geq 420$ nm). They attributed this enhancement to the good distribution of CdSe nanoparticles on TiO_2 nanorod arrays, the favorable band alignment, and the intimate interfacial interaction between CdSe nanoparticles and TiO_2 nanorods.

Based on literature, the electrodeposition of CdSe onto TiO_2 films could be applied from various types of electrolytes including aqueous solutions [31-36], organic solutions [37] or ionic liquid medium. In fact, ionic liquids are molten salts with melting points often around 20–25 °C or below, composed only

of ions. As compared to acqueous and organic electrolytes, ionic liquids are much preferred thanks to its high thermal and good electrochemical stability (> 300 ◦C) Which permitting the electrodeposition to be proceeded even at high temperatures allowing atom diffusion on the surface during growth. It has crucial positive impact on the quality of the resulted layers. ILs exhibit good solvating properties, high conductivity, non-volatility, low toxicity and wide electrochemical potential window. The viscosity of ionic liquids causes a slowdown electrocoating giving a more homogeneous and compact thin films. Another important advantage of ILs based electrolyte is the absence of hydrogen evolution simultaneously with metal deposition that often occurs during electrodeposition in aqueous solution. This phenomenon has a deep effect not only on photocurrent efficiency but also on the final quality of deposited layer. Thus, Ionic liquids (ILs) were considered as an appropriate alternative electrolytes for the electrodeposition of CdSe onto TiO_2 thanks to their intrinsic physico-chemical properties [38,39]. Actually, There are no published work reported the effect of the ionic liquid based electrolyte or ionic liquid/ organic solvent based electrolyte medium on the PEC performance of electrodeposited CdSe films on to TiO_2 films.

In this work, we report for the first time ever on the simple and low cost electrochemical deposition strategy of CdSe onto sol-gel prepared TiO_2 thin film from Tricaprylmethylammonium chloride/Formamide based electrolyte as eventual mixture of (Ionic Liquid/ Organic Solvent) medium. Then, the effect of TiO2 sensitization with the electrodeposition of CdSe layer on structural, optical, photoelectrochemical and photocatalytic properties has been deeply investigated.

Experimental Details

Materials

All chemicals were of analytical reagent grade, purchased from Sigma Aldrich and were used without further purification. Aqueous solutions were prepared using deionized water. Sol-gel via spin coating method was adopted to deposit the TiO_2 thin films onto ITO conductive glass substrates. Prior to use, all substrates were ultrasonically cleaned during 15 min with consecutively acetone and iso-propanol, rinsed with deionized water, and finally dried in air at room temperature. The CdSe was deposited by electrodeposition technique on TiO_2 electrode

Preparation method of TiO_2

TiO_2 thin films were prepared using sol–gel process and then deposited on ITO glass. Titanium isopropoxide $Ti(OCH(CH_3)_2)_4$ was used as a TiO_2 source. The sol was a mixture, in a molar ratio, of titanium isopropoxide, as a precursor, isopropanol $CH_3CH(OH)–CH_3$ and methanol CH_3OH, as solvents and acetic acid CH_3COOH as a catalyst. First, 1.5 mL of $Ti(OCH(CH_3)_2)_4$ was dissolved in 4.5 mL of isopropanol. The solution was homogenized for 30 min under magnetic stirring while heating up to 60 °C. Then 4 mL of acetic acid was added, with stirring for 30 min under the same heating. Finally, heating was stopped and 12 mL of methanol was added. The mixture was held under the magnetic stirring for 2 h. The TiO_2 was deposited onto (ITO)-coated glass substrates by using spin coating technique. The spinning speed was set at 3000 rpm and the deposition time to 30 s. The TiO_2 solution was dropped one time onto the substrate and then dried in the oven at 100 °C for 10 min; The drying process was repeated three times and the resulted samples have been annealed at 450 °C for 2h.

Electrodeposition of CdSe onto TiO_2 thin film

CdSe sensitized layer was electrodeposited onto the annealed TiO_2 thin film at room temperature under agitation from an electrolyte composed of 30 % aliquat 336 (TOMAC) and 70 % formamide, 10^{-2} M SeO_2, 10^{-2} M $CdCl_2$ and 0.1 M KCl. The electrodeposition was carried out via three-electrodes system (Voltlab PGZ 100) containing TiO_2 film as working electrode, Ag/AgCl as a reference electrode, and Pt as a counter electrode. During the electrodeposition, the electrolyte was continuously stirred at a moderate speed with the help of a magnetic stirrer. The deposition potential was fixed at a constant voltage -1.1 volt for about 15 minutes. Finally, the resulted CdSe/TiO_2 heterostructure was annealed at 250 °C for 30 min in nitrogen atmosphere.

Characterization of bareTiO_2 and CdSe/TiO_2 thin films

The samples were characterized by X-ray diffraction (XRD) using Bruker D8 advance X-ray diffractometer with CuK_α (λ = 1.541 Å) radiation for 2θ values in the range of 10–80 °. A Raman scattering study was performed on a Jobin Yvon Lab RAM HR spectrometer using 632.8 nm irradiation from a He–Ne laser at (3 mW). Surface morphology of the prepared films was characterized via Atomic Force Microscopy (AFM)

(Nano-scope III) in tapping configuration and using a field-emission scanning electron microscope (FE-SEM, JSM-5410, JEOL). Accelerating voltage of SEM was set to 20 kV. Optical absorption A (λ) of the films was measured by a UV–vis–NIR (Lambda 950) spectrophotometer, equipped with an integrating sphere, in the wavelength range 300–800 nm. Bare TiO_2 and CdSe/TiO_2 thin films were also characterized by room-temperature photoluminescence spectra (PL) on a PL fluorescence spectrometer (Perkin-ElmerLS55) using a Xe lamp with an excitation wavelength of 300 nm.

Photoelectrochemical measurements

The PEC splitting performance measurements were carried out in a quartz electrolytic cell. The sample (with an average area of 1 cm^2), a Pt plate (with an average area of 1 cm^2), and an Ag/AgCl electrode were employed as the working electrode, counter electrode and reference electrode respectively. The electrolyte was composed of 0.5 M sodium sulfate aqueous solution. Current densities, as a function of applied potential (-1 to + 0.5 V vs. Ag/AgCl electrode) for the samples, were recorded under front-side illumination with a computer-controlled Potentiostat/Galvanostat PGSTAT30 (Eco Chemie BV) for all PEC experiments. A 300 W Xe short arc lamp passing through an AM 1.5 G filter Model-SS80AA with white light intensity of 100 mW/cm^2 was employed to simulate solar light. The intensity of incident light from the Xe lamp was measured using a Photometer Model 70310 from Spectra-Physics.

Key Findings

Electrochemical Growth

In order to determine the deposition potential of CdSe, a systematic cyclic voltammetry study was undertaken on ITO and TiO_2/ITO working electrodes from ionic liquid based electrolyte (Figure 1). The potential started at the open circuit potential and was initially swept towards the negative direction at a scan rate of 20 mV/s. From Figure 1(a), three cathodic peaks are clearly seen in the voltammogram at about -0.6 V, -0.9 V, and -1.1V versus Ag/AgCl reference electrode

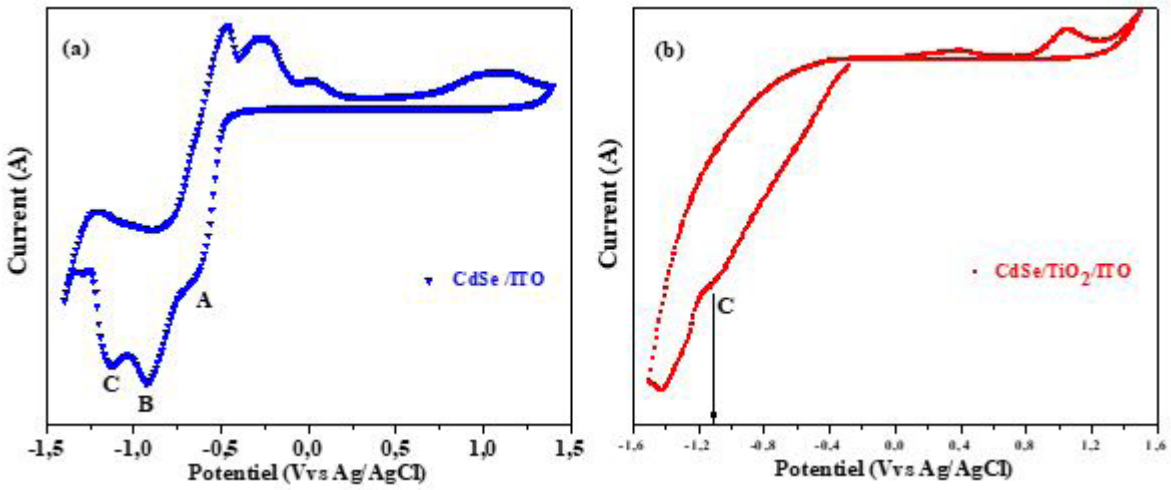

Figure 1: Cyclic voltammograms recorded for binary Cd-Se system from ionic liquid solution composed of 30 % aliquat 336 (TOMAC) and 70 % formamide, 10^{-2} M SeO_2, 10^{-2} M $CdCl_2$ and 0.1 M KCl deposited on a) ITO glass substrate, b) ITO/TiO_2 working electrodes

The deposited cadmium selenide was attributed to the following reactions:

$$SeO_2 + H_2O \rightarrow H_2SeO_3$$

$$H_2SeO_3 + H^+ + 6e^- \rightarrow H_2Se + 3\,H_2O \quad \text{peak } A_1$$

$$H_2SeO_3 + H_2Se + 2H^+ + 2e^- \rightarrow 2Se^0 + 3H_2O \quad \text{peak } A_2$$

$$Se^0 + Cd^{2+} + 2e^- \rightarrow CdSe \quad \text{peak } A_3$$

At the beginning, the H_2SeO_3 (aq) was reduced into H_2Se (aq) soluble species. The reduction of H_2Se (aq) to Se^0 was started from -0.75 V and reached the peak value at about -0.9 V. Finally, the electrodeposition mechanism of CdSe thin film onto ITO coated glass substrate took place at a potential of -1.1 V versus Ag/AgCl wherein Cd^{2+} was reduced to Cd on the surface of the substrate. Hence, the CdSe alloy was formed according the potential deposition mechanism [40].

Figure 1 (b) displays the cyclic voltammogram (CV) of electrodeposited CdSe onto TiO_2/ITO working electrode from ionic liquid based electrolyte. Obviously, only one main cathodic peak at about -1.1 V versus Ag/AgCl was noted. The change of the cyclic voltammogram CV was attributed to the change in the working electrode's surface. As compared with Figure 1(a), this main reduction peak was certainly assigned to the electrodeposition of CdSe thin film.

In order to confirm this assumption, the potentiostatic cathodic electrodeposition was conducted at the potential of -1.1 V versus Ag/AgCl onto sol-gel coated TiO_2/ITO film. The deposited film was therefore annealed at 250 °C for 30 min in N_2 atmosphere and was analyzed by XRD and RAMAN measurements.

Structural study

Figure 2 exibits the XRD patterns of bare TiO_2 and CdSe/TiO_2 samples. The sol-gel prepared TiO_2 layer onto ITO glass substrate via spin coating approach shows a main peak at 25.35 ° which was assigned to (101) plane and attributed to the anatase phase with tetragonal crystal structure of TiO_2 (JCPDS #89-4921). This result is in agreement with those published in the literature [41]. The electrodeposition of CdSe onto TiO_2/ITO substrate at an applied potential of -1,1 V from the ricaprylmethylammonium chloride/Formamide based electrolyte, additional characteristic peaks have appeared at 2θ = 25.5 °, 35.2 °, and 41.9 ° which were attributed to (002), (102) and (110) planes respectively. These noticeable planes were ascribed to the hexagonal structure of CdSe according to the card number (JCPDS # 65-3415) verified by JCPDS (Joint Committee on Powder Diffraction Standards) database. This structural study reveals that the hybride CdSe/TiO_2 nanostructure has been successfully prepared by the low cost and facile electrodeposition approach at the applied potential of -1.1 V.

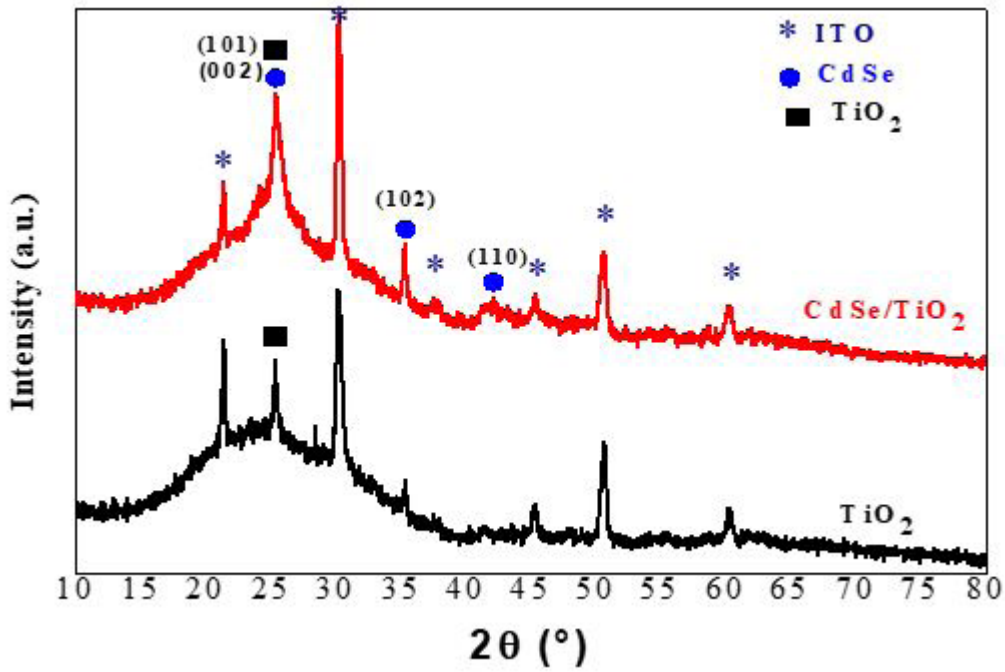

Figure 2: X-ray diffraction patterns of bare TiO_2 and CdSe/TiO_2 thin films

Raman study

The Raman spectra of bare TiO_2 and CdSe/TiO_2 films in the range of 100 cm^{-1} to 550 cm^{-1} are shown in Figure 3. Sol-gel coated TiO_2 spectrum reveals three symmetric vibration modes; A_{1g}, B_{1g} and E_g attributed to the tetragonal anatase phase of TiO_2. They were identified at 144 cm^{-1} for E_g mode, 396 cm^{-1} for B_{1g} mode and 516 cm^{-1} for A_{1g} vibrational mode respectively [42]. The electrodeposition of CdSe onto TiO_2 film resulted in the decrease of anatase characteristic peak intensity of TiO_2 (E_g) due to the surface recovery of TiO_2. In addition, two new peaks have appeared at 203 cm^{-1} and 406 cm^{-1} corresponding to the longitudinal optical (LO) and to the second harmonic (2 LO) respectively of CdSe [43]. Those Raman results confirm those obtained by XRD study.

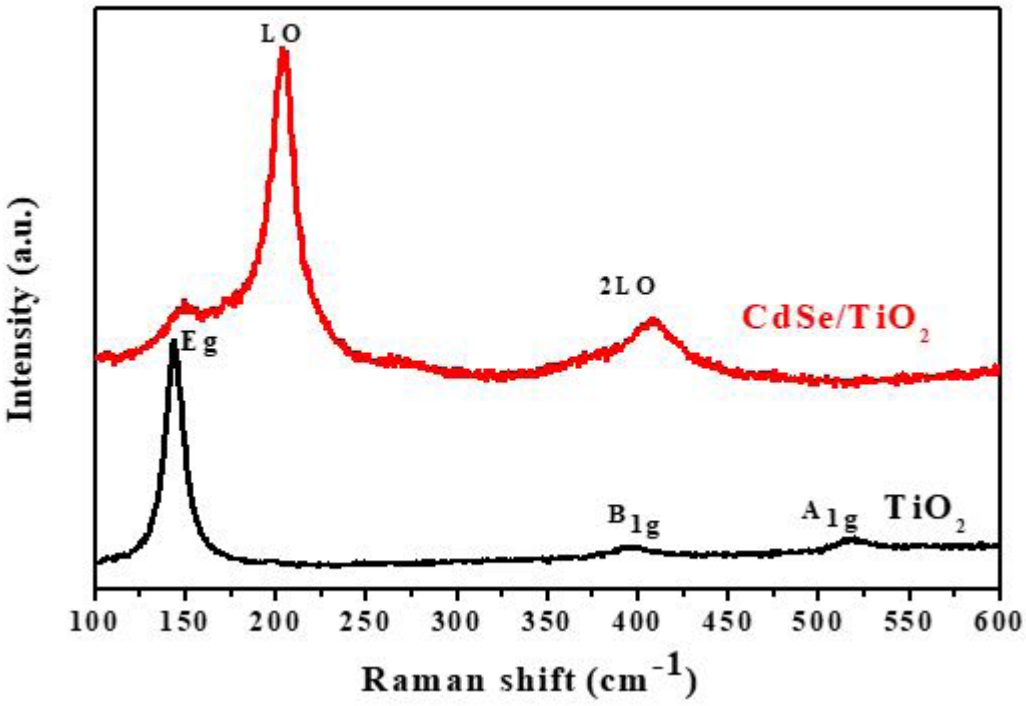

Figure 3: Raman spectra of TiO_2 and $CdSe/TiO_2$ based thin films

Morphological studies

Figure 4 shows the morphology of bare TiO_2 and $CdSe/TiO_2$ films by Atomic Force Microscopy (AFM) and Scanning Electron Microscopy (SEM). The surface of sol-gel coated TiO_2 film was dense, homogeneous and covered with well distributed small spherical shaped grains showing the general characteristic morphology of the anatase phase [44]. However, the surface topography has changed after the electrodeposition of CdSe which could be attributed to the CdSe deposited layer onto TiO_2 thin film. The root mean square (RMS) surface roughness of nude TiO_2 thin film has increased from 1.08 nm to 38.833 nm after electrodeposition of CdSe. The increase in the film roughness has proved the growth of electrodeposited CdSe onto nanostructured TiO_2 based thin film. In order to confirm this AFM results, SEM topography has also been investigated in Figure 4.

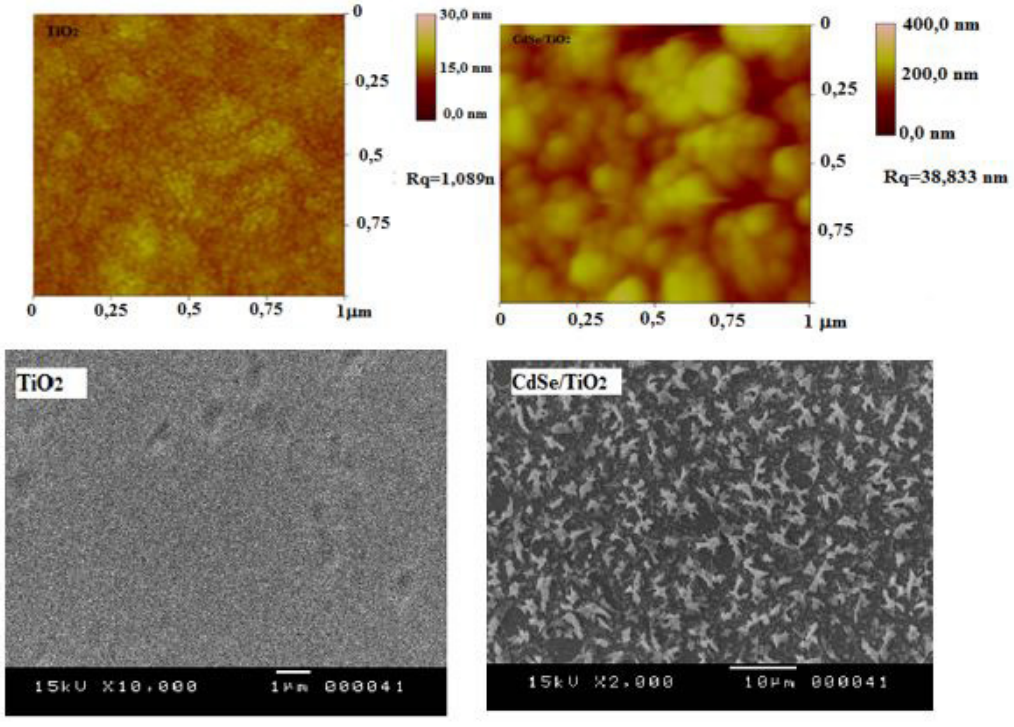

Figure 4: 2D AFM and SEM images of TiO_2 and $CdSe/TiO_2$ elaborated thin films

SEM image of bare TiO_2 layer reveals that the surface was clearly filled with granular shapes. After CdSe electrodeposition, the morphology has changed and consists of agglomerated small grains well distributed on the TiO_2 surface resulted in the growth of CdSe film.

Optical properties

UV-Visible absorption spectra of TiO_2 and CdSe/TiO_2 thin films are shown in Figure 5. The bare TiO_2 has an absorption edge at around ~375 nm, showing a fundamental absorption edge which corresponds to the TiO_2 band gap energy of anatase structure (3.2 eV) in the ultraviolet region [45, 46]. The electrochemical deposition of CdSe onto TiO_2 has obviously extended the absorption spectrum to the visible light region. The narrow band-gap of photoabsorber CdSe was responsible for the improved absorption capability of TiO_2 thin film in the visible-light region and consequently enhances its photocatalytic and photoelectrochemical performances [47].

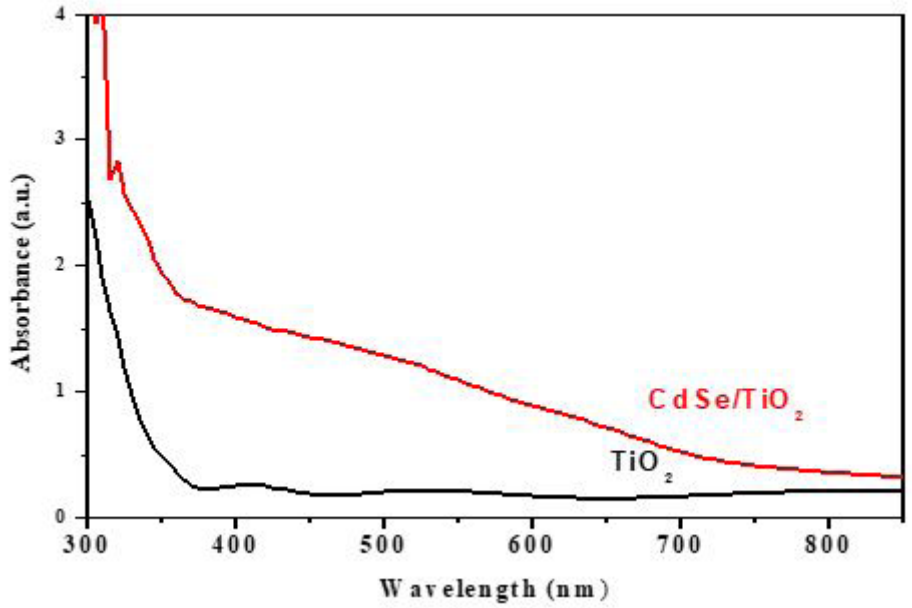

Figure 5: UV–vis absorption spectra of TiO_2 and CdSe/TiO_2 thin films

The charge separation and transfer mechanism was revealed by measuring the electron injection efficiency by photoluminescence (PL) spectroscopy as shown in Figure 6. Through an excitation wavelength of 300 nm, the CdSe based photosensitizer exhibited a characteristic emission peak situated at 600 nm which corresponds to the recombination of the excited electrons. Whereas, the PL signal disappears with sensitization of TiO_2 with CdSe. This PL quenching reveals the decrease in the rate of excited electrons which get recombined radiatively with the holes situated in CdSe valance band. Therefore, it can be concluded that most of the excited electrons are successfully injected into the TiO_2 conduction band [48-51].

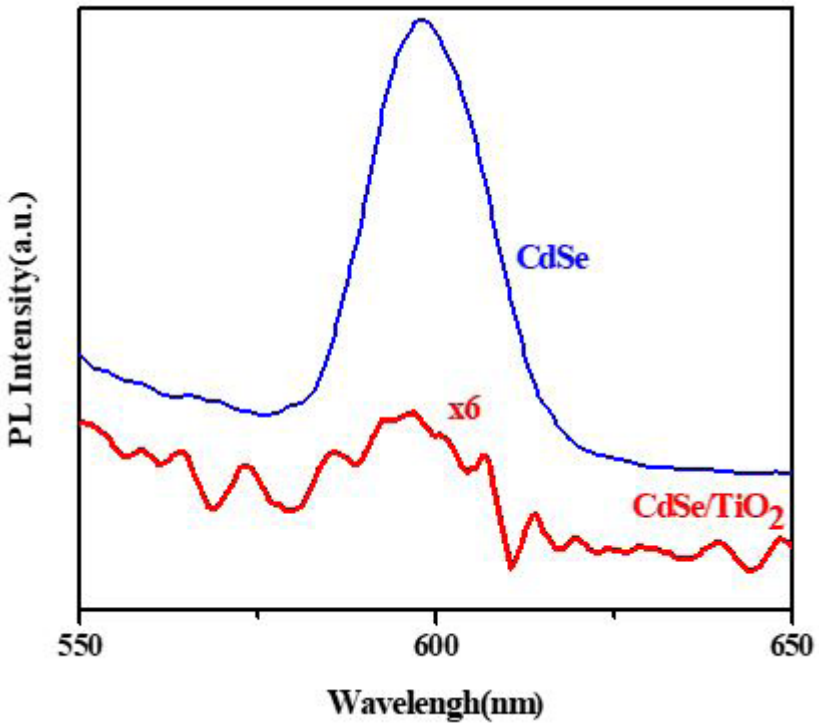

Figure 6: Photoluminescence spectra of CdSe and CdSe/TiO_2 thin films

According to the literature, photoluminescence spectroscopy confirms the presence of the type-II interfacial transition between the valence band of CdSe and the conduction band of TiO_2 [52, 53] thanks to its energy levels shown in Figure 7. [52-54]. This PL results suggest that electrodeposition of CdSe onto TiO_2 photoelectrode enhances the charge separation

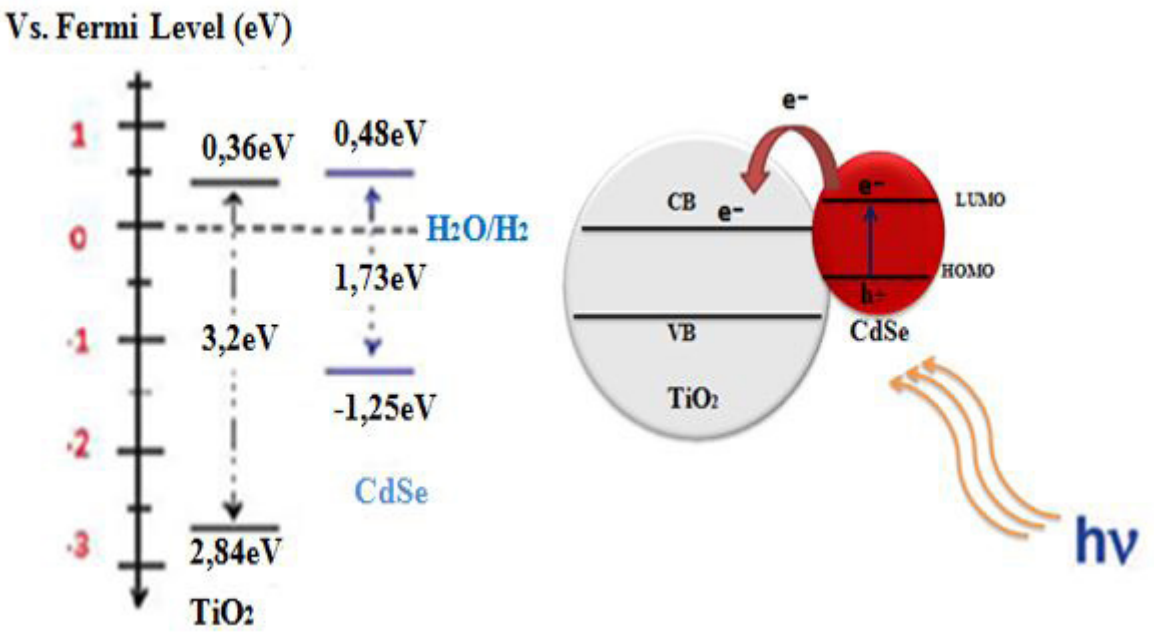

Figure 7: Energy levels diagram and schematic illustration of the injection of electrons from the CdSe conduction band to that of the TiO_2.

Photoelectrochemical properties

The linear sweep voltammogram (LSV) is a useful technique evaluate the charge carrier characteristics at the semiconductor/electrolyte interface by evaluating the separation efficiency of photogenerated electron-hole pairs. In order to investigate the impact of the photosensitization of TiO_2 with CdSe on the separation efficiency of photogenerated electron–hole pairs, we expose the elaborated photoanodes to a photocurrent response measurements. Figure 8 (A) and Figure 8(B) show current density-voltage (J–V) measurements of TiO_2 and CdSe/TiO_2 photoanodes in dark and under illumination with 100 mW/cm^2 from Xenon lamp in aqueous solution containing 0.5 M Na_2SO_4 (pH=7) with applied potential ranging from -1 to 0.5 V (vs. Ag/AgCl).

It is clearly seen in Figure 8 (A) that there is no dark photocurrent for both photoelectrodes.

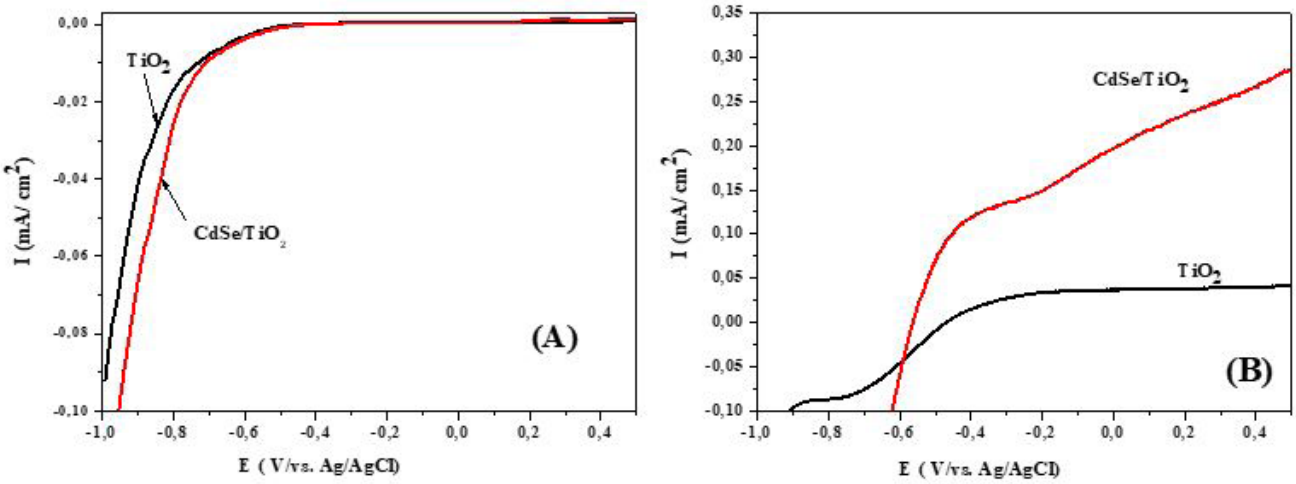

Figure 8: Photocurrent density plots of TiO_2 and CdSe/TiO_2 photoanodes in dark (A) and under illumination (100 mW/ cm^2) (B)

According to a literature survey, this result could be explained by the presence of the TiO_2 based compact film that plays an effective role in blocking the direct contact between the electrolyte and ITO substrate which suppresses the leakage photocurrent [54]. The use of TOMAC/FA as ionic electrolyte in the electrodeposition of CdSe onto TiO_2/ITO substrate has a crucial positive impact on the quality of the resulted photoanodes by improving the compactness of the film [54]. Under illumination, the increase at applied voltage (V vs.Ag/AgCl) promotes the separation of photo-generated charges and the photo-current density (JSC) has increased [55, 56]. All samples have a common behavior; a photocurrent flowed in the positive potentials and increased gradually which is the characteristic of n-type semiconductor.

Moreover, low photocurrent was observed for the both photoanodes. This may be explained by the fast recombination of the photogenerated electrons and holes. Similar behavior was also reported by others authors [57,58]. Under illumination, bare TiO_2 presents a photocurrent density of 0.04 mA/cm^2 at 0.5 V which is comparable to that reported by Ayal et al [34], in CdSe-sensitization of TiO_2 nanotube arrays through electrodeposition approach. They have found a 0.03 mA/cm^2 as photocurrent density for bare TiO_2.

As compared to TiO_2 layer, the photocurrent density of hybrid CdSe/TiO_2 heterostructure was greatly enhanced and reached a value of 0.30 mA/cm^2 at 0.5 V which is 7.5 times higher than bare TiO_2 We have also noticed from Figure 10(B) that CdSe/TiO_2 PA shows a more negative zero-current potential (-0.56V) than that of the bare TiO_2 thin film (-0.46 V). These results could be explained through the high absorption and the better charge separation efficiency of the photogenerated carriers [59]. These results are consistent with the Photoluminescence results. This suggests that the electrodeposition of CdSe on TiO_2 thin film has improved the generation and separation of photoinduced charges.

Figure 9 shows the PEC water splitting device for the CdSe/TiO_2 PA. Through coupling the two semiconductors, most of the excited electrons have been successfully injected from the CdSe conduction band into that of TiO_2. This reduces the photogenerated carriers recombination rate in TiO_2. Consequently, it facilitates the transport of electrons to the platinum electrode through the external circuit to participate in the reduction of protons at the interface between the cathode and the electrolyte leading to the formation of hydrogen gas. Meanwhile, the holes generated vacancies and contribute to the

oxidation of water by producing oxygen at the interface between the photoanode and the electrolyte. This PEC water splitting mechanism undergo the following steps:

$CdSe/TiO_2 + h^+ \rightarrow CdSe\ (h^+, e^-)/TiO_2$ (1)

$CdSe\ (h^+, e^-)/CdSe \rightarrow CdSe\ (h^+)\text{-}TiO_2\ (e^-)$ (2)

$TiO_2\ (e^-) \rightarrow Pt\ (e^-) + TiO_2$ (3)

$H_2O + CdSe\ (h^+) \rightarrow ½\ O_2 + 2H^+ + CdSe$ (4)

$Pt\ (e^-) + 2H \rightarrow Pt + H_2$ (5)

According to the (J-V) curve under illumination, the corresponding photoconversion efficiency, the applied bias photon-to-current efficiency (ABPE) was calculated via the following equation [60] and presented in Figure 10.

$$\eta\ (\%) = J_{sc}\ [E°rev- |E_{app}|/I_{Light}]*100 \quad (6)$$

where η is the photoconversion efficiency, J_{sc} is the photocurrent density (mA/cm^2), I_{Light} is the incident light, $E°_{rev}$ is the standard reversible potential which is 1.23 V RHE, and E_{app} is the applied potential which is $E_{app} = E_{meas} - E_{aoc}$, where E_{meas} is the electrode potential (vs Ag/AgCl) of the working electrode and E_{aoc} is the electrode potential (vs Ag/AgCl) of the same working electrode under open circuit and under illumination conditions.

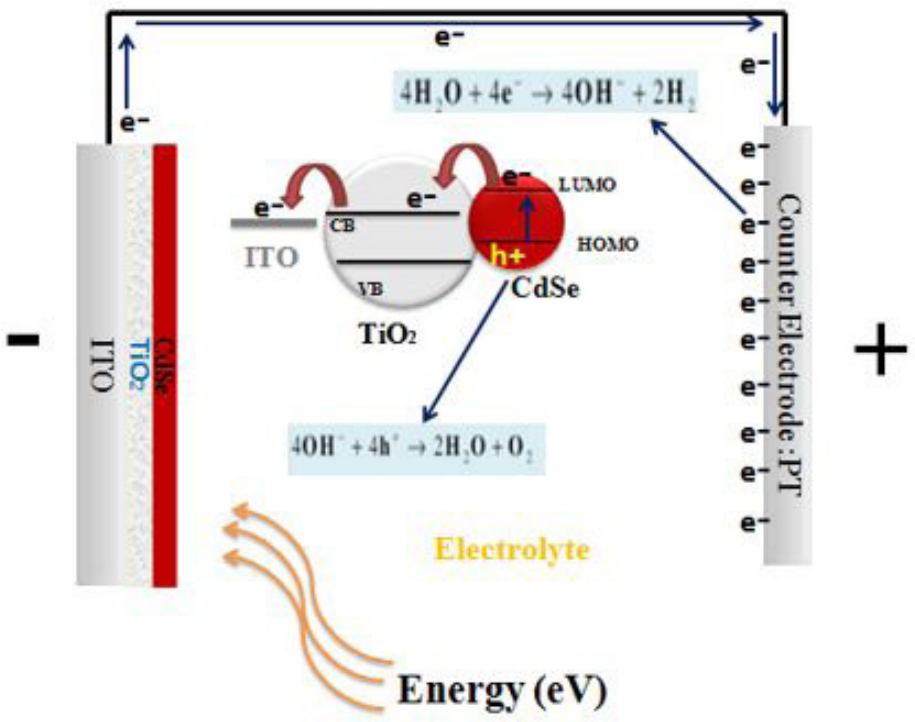

Figure 9: Schematic illustration of the PEC water splitting for the $CdSe/TiO_2$ photoelectrode

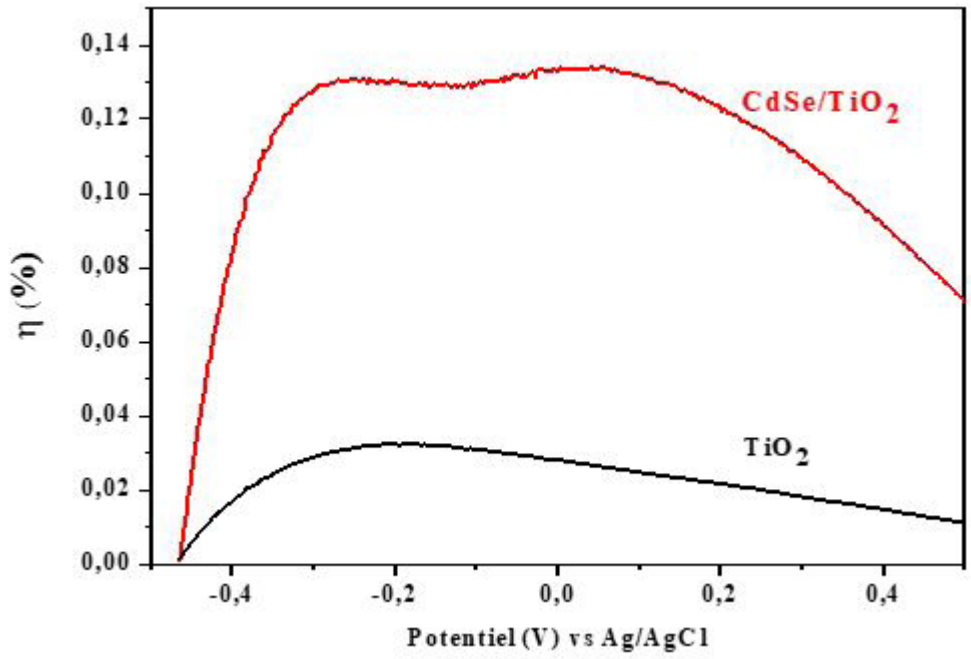

Figure 10: Photoconversion efficiency of bare TiO_2 and $CdSe/TiO_2$ photoanodes as a function of applied potential

The PEC parameters including open-circuit voltages (V_{oc}), short-circuit current density (J_{sc}), fill factor (FF) and power conversion efficiency (η) were tabulated in Table 3.

Table 3: PEC performance of the TiO_2 photoelectrode and the heterostructured $CdSe/TiO_2$ photoelectrode designed for water splitting under 100 mW/cm^2 from Xenon visible light

	J_{SC} (mA/cm²)	V_{oc} (V)	FF	η (%)
TiO_2	0.04	-0.47	0.39	0.03
$CdSe/TiO_2$	0.20	-0.56	0.43	0.13

Typically, the $CdSe/TiO_2$ photoanode shows higher conversion efficiency of 0.13 % at -0.2 V (vs Ag/AgCl) which is ~ 4.3 times higher than that of pure TiO_2 layer (0.03 %). The enhanced photoconversion efficiency could be assigned to the improvement in incident light absorption and the ameliorated separation rate of photogenerated charges.

In order to investigate the stability and the reproducibility of the device's phtoresponse, the photocurrent-time (J-t) plots of TiO_2 and $CdSe/TiO_2$ photoanodes have been measured at an applied potential of 0 V and displayed in Figure 11. The photocurrent of elaborated samples appeared immediately upon irradiation then quickly returned to a steady state when the illumination was cut off. These results indicate the stability of the samples and the immediate generation and separation of electron (e-)/hole (h+) pairs in TiO_2 and $CdSe/TiO_2$ based photoanodes [61]. It is worth noty that the CdSe sensitized TiO_2 photoanode yields a photocurrent density of 0.28 mA/cm^{-2} which is about 9.5 times higher than that reached with bare TiO_2 (0.029 mA/cm^{-2}). These results indicated that the sensitization of TiO_2 with CdSe can clearly enhance the transient photocurrent responses which confirm the observed trends in Figure 8.

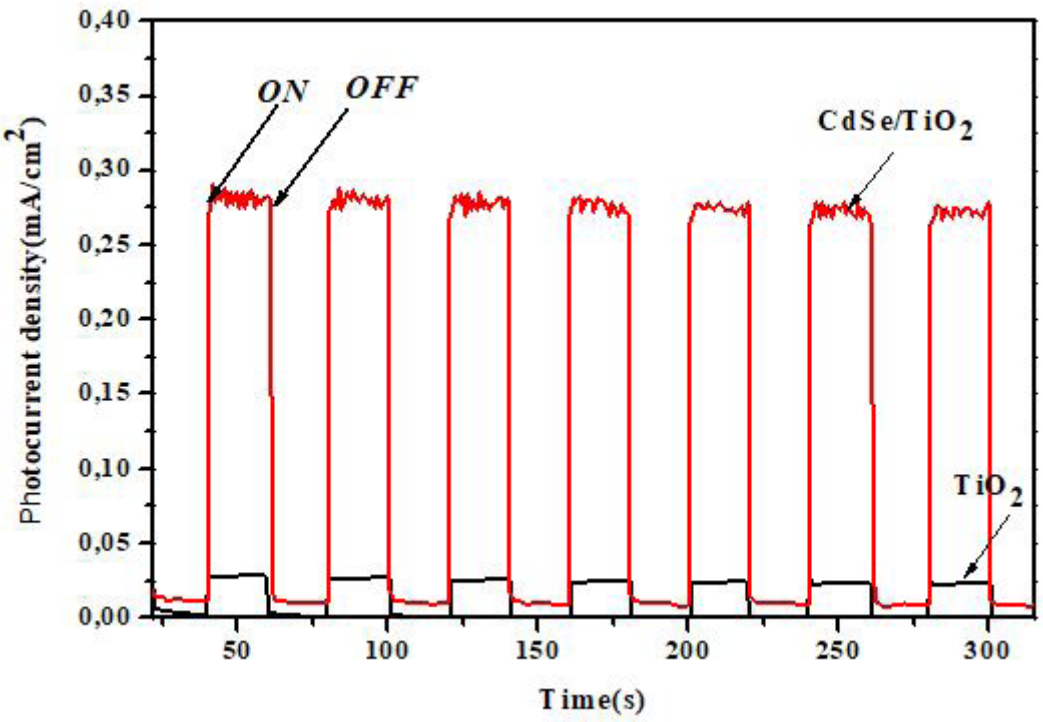

Figure 11: Photocurrent density-time response of TiO_2 and $CdSe/TiO_2$ photoanodes under illumination (100 mW/cm^2) at an applied potential of 0 V (vs Ag/AgCl)

Photocatalytic activities

The discharge of untreated wastewater from various industries causes serious environmental pollution and threatens the human and ecosystem well-being. Thus, Methylene blue MB and methyl MO containing wastewater should be decolorized and detoxified before being discharged into the environment since they are potential carcinogen dyes [60-62].

The photocatalytic activities of synthesized photocatalysts were carried out by the degradation of MB and MO dyes under visible light irradiation and illustrated in Figure 12. It is clearly seen that the maximum absorbance of MB and MO dyes situated at 660 nm and 484 nm respectively have sharply decreased in the presence of TiO_2 and CdSe/ TiO_2 based catalysts. These results show that the photocatalytic degradation efficiency of TiO_2 has improved after photosensitization with CdSe. This improvement originated from the enhanced absorption capability and the efficient charge separation [65]. Figure 13.

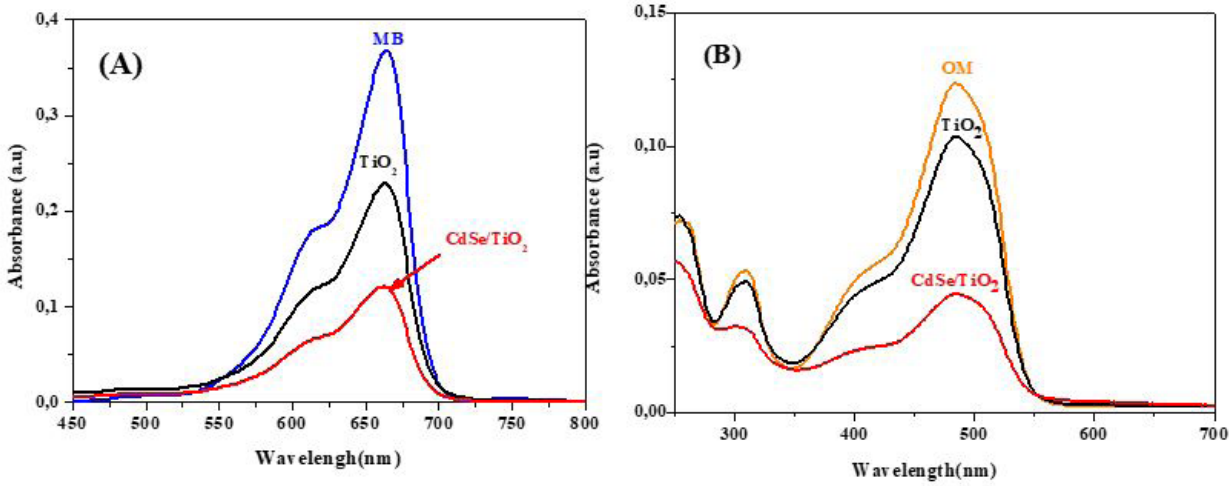

Figure 12: Absorption spectra of Methylene blue (a) and Methyl orange (b) solutions obtained after 2 h in the presence of TiO_2 and with $CdSe/TiO_2$ photocatalysts

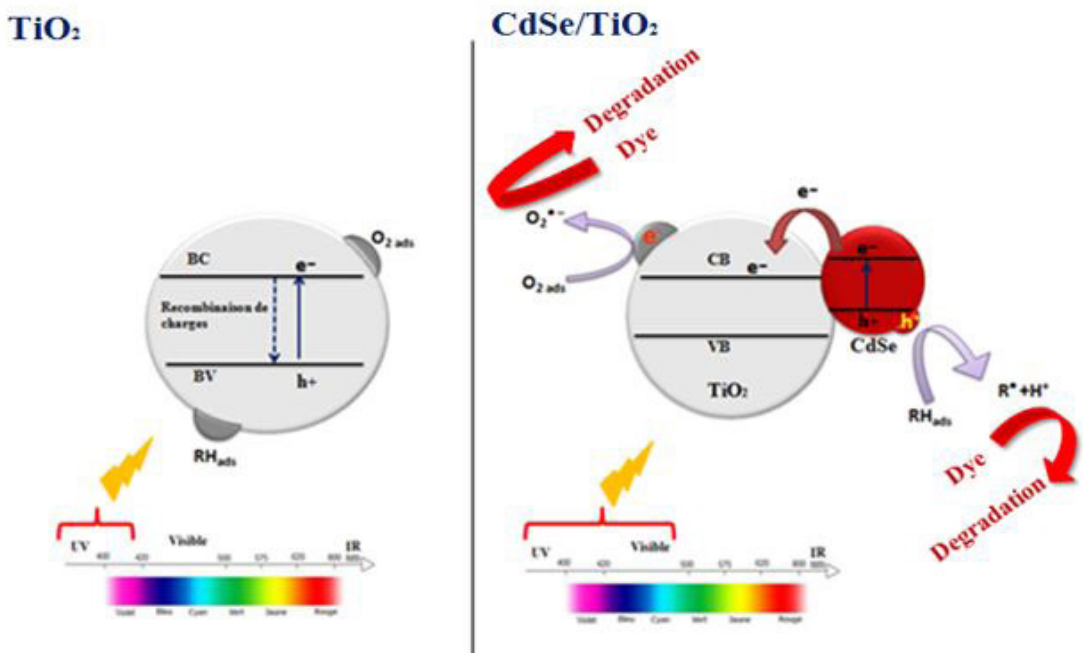

Figure 13: Schematic illustration of the photocatalytic degradation mechanism with TiO2 and with CdSe/TiO2 photocatalysts

Conclusion

In summary, the sensitation of TiO_2 with short band gap CdSe absorber has successfully provided through the low cost, facile and eco-friendly electrochemical deposition. It has been demonstrated that this electrochemical approach via the use of TOMAC/FA based electrolyte has a crucial role in the high stability and compactness of sol-gel synthesized TiO_2 layers.

Structural study proved the cyclic voltammetry synthesis of hybride CdSe/TiO_2 nanostructure at the applied potential of -1.1 V with well-defined phases. Meanwile, raman results confirm those obtained by XRD investigation by exhibiting the characteristic peaks for the anatase type TiO_2 and hexagonal phase of CdSe respectively. AFM morphological study of bare TiO_2 layer shows a dense, homogeneous and a surface covered with well distributed small spherical shaped grains. Its root mean square (RMS) surface roughness has rised from 1.08 nm to 38.833 nm after electrodeposition of CdSe which is a good proof for the successful growth of electrodeposited CdSe onto nanostructured TiO_2 based thin film via the TOMAC/FA medium.

In order to confirm this AFM results, SEM image of bare TiO_2 layer reveals that the surface was clearly filled with granular shapes. After CdSe sensitization, the morphology has been modified and consisting of agglomerated well distributed small grains on the surface of TiO_2 resulted in the growth of CdSe film. As compared to bare TiO_2, optical measurements show better charge separation efficiency for the CdSe/TiO_2 heterostructure. The sensitization with CdSe has resulted in enhanced photocurrent density of 0.30 mA/cm^2 at 0.5 V which is 7.5 times higher than bare TiO_2 when exposed to visible light irradiation. In terms of conversion efficiency, CdSe/TiO_2 photoanode shows higher conversion efficiency of 0.13 % at -0.2 V (vs Ag/AgCl) which is ~ 4.3 times higher than that of bare TiO_2 layer. Also, CdSe/TiO_2 PA shows a zero-current potential of -0.56 V which is more negative than that of bare TiO_2 thin film (-0.46 V). The sensitization process of TiO_2 with CdSe from the ionic liquid has improved photocatalytic degradation efficiency of TiO_2 towards MB and MO pollutant dyes thanks to the amelioration of its absorption capacity and charge separation rate of photogenerated carriers. The sensitization of TiO_2 with CdSe from TOMAC/FA based ionic liquid medium has resulted in low cost and high stable CdSe/TiO_2 photoanode for PEC solar cells and photocatalytic degradation applications and consequently overcome the serious environmental issues

Acknowledgments

This work was supported by the Ministry of Higher Education and Scientific Research of Tunisia.

Conflicts of Interest

The authors declare no conflict of interest.

References

1. Fujishima A, Honda K (1972) Nature 238: 37-38.

2. Michael A, Henderson A (2011) Surf Science Reports 66: 185-278.

3. Kim HS, Jung SW, Yang SK, Ahn KS, Kang SH (2013) Mater Lett 111: 47-50.

4. Huang JY, Zhang KQ, Lai YK (2013) Int J Photoenergy 2013: 761971.

5. Mor GK, Varghese OK, Paulose M, Shankar K, Grimes CA (2006) Sol Energy Mater Sol Cells 90: 2011-2075.

6. Zhuang H, Miao J, Huang H, et al. (2015) Chem Phys Chem 16: 1352-1355.

7. Zhao H, Chen Y, Quan X, Ruan X (2007) Chinese Science Bulletin 52: 1456-1461.

8. Lin HJ, Yang TS, His CS, Wang MC, Lee KC (2014) Ceramics International 40: 10633-10640.

9. Tu YF, Huang SY, Sang JP, Zou XW (2009) Journal of Alloys and Compounds 482: 382-387.

10. Yang H, Pan C (2010) Journal of Alloys and Compounds 501: 8-11.

11. Ma H, Fan Q, Fan B, et al. (2018) Langmuir 34: 7744-7750.

12. Luo Z, Qi Q, Zhang L, Zeng R, Su L, Tang D (2019) Anal Chem 91: 4149-4159.

13. Kang Q, Liu S, Yang L, Cai Q, Grimes CA (2011) ACS Applied Materials & Interfaces 3: 746-749.

14. Y. Lu, G. Yi, J. Jia, Y. Liang, Applied Surface Science 256 (2010) 7316-7322.

15. Z. Zhou, J. Fan, X. Wang, W.Sun, W. Zhou, Z. Du, S. Wu, ACS Applied Materials & Interfaces 3 (2011) 2189-2194

16. Aiyun Meng, Liuyang Zhang, Bei Cheng, Jiaguo Yu (2019) Advanced materials 31.

17. Chin Wei Lai, Nurul Asma Samsudin, Foo Wah Low, Nur Azimah Abd Samad, Kung Shiuh Lau, et al. (2020) Materials 13: 25-33.

18. Hou J, Zhao H, Huang F, Jing Q, Cao H, Wu Q, Peng S, Cao G (2016) J Power Sources 325: 438-445.

19. Salunkhe DB, Dubal DP, Sali JV, Sankapal BR (2015) Ceram Int 41: 3940-3946.

20. Zhao F, Tang G, Zhang J, Lin Y (2012) Electrochim. Acta 62: 396-401.

21. Zhu G, Pan L, Xu, Zhao Q, Lu B, Sun Z (2011) Nanoscale 3: 2188-2193.

22. Shen Q, Yamada A, Tamura S, Toyoda T (2010) Appl Phys Lett 97: 123-107.

23. Barea EM, Shalom M, Gimenez S, Hod I, Mora-Sero I, Zaban A, et al (2010) J Am. Chem Soc 132: 19.

24. Yu L, Li Z, Liu Y, Cheng F, Sun S (2014) J Power Sources 270: 42-52.

25. Fang B, Kim M, Fan SQ, Kim JH, Wilkinson DP, et al. (2011) J Mater Chem 21: 8742-8748.

26. Liu D, Liu J, Liu S, Wang C, Ge Z, et al. (2019) J Mater Sci 54: 4884-4892.

27. Unni GE, Deepak TG, Nair AS (2016) Mater Sci Semicond Process 41: 370-377.

28. Wang R, Wan L, Niu H (2013) J Sol-Gel Sci Technol 67: 458-463.

29. Zhang Y, Zhu J, Yu X, Wei J, Hu L, Dai S (2012) Sol Energy 86: 964-971.

30. Chong LW, Chien HT, Lee YL (2010) J Power Sources 195: 5109-5113.

31. Wang W, Li F, Zhang D, Leung DYC, Li C (2016) Photoelectrocatalytic hydrogen generation and simultaneous degradation of organic pollutant via CdSe/TiO2 nanotube arrays. Applied Surface Science. 362: 490-497.

32. Ayal AK, Zainal Z, Lim HN, Talib ZA, Lim Y-Chin, Keng CS, Holi AM (2018) Fabrication of CdSe nanoparticles sensitized TiO2 nanotube arrays via pulse electrodeposition for photoelectrochemical application. Materials Research Bulletin. 106: 257-262.

33. Jinbo Xue, Qianqian Shen, Wei Liang, Xuguang Liu, Fei Yang (2013) Electrochimica Acta 97: 10-16.

34. Asmaa Kadim Ayal, Zulkarnain Zainal, Hong-Ngee Lim, Zainal Abidin Talib, et al. (2016) J Mater Sci: Mater Electron 27: 5204-5210.

35. Jinbo Xue, Qianqian Shen, Fei Yang, Wei Liang, Xuguang Liu (2014) Journal of Alloys and Compounds 607: 163-168.

36. Asmaa Kadim Ayal, Zulkarnain Zainal, Hong-Ngee Lim, Zainal Abidin Talib, Ying-Chin Lim, et al. (2017) Opt Quant Electron 49: 164.

37. Huaqiang Zhuang, Xiaobin Liu, Fukun Li, Wentao Xu, Liqin Lin, Zhenping Cai (2019) Int J Energy Res. 43: 7197-7205.

38. Dipal B, PatelaKhushb, Chauhan Mukhopadhyay R (2019) Journal of Electroanalytical Chemistry 847: 113-233.

39. Shibin Thomas, Jeremy Mallet, Hervé Rinnert and Michael Molinari (2018) RSC Adv 8: 3789.

40. Ibtissem Ben Assaker, Halima Elbedoui, Radhouane Chtourou (2012) Electrochimica Acta. 81: 149-154.

41. Tu Y, Wu J, Zheng M, Huo J, Zhou P, Lan Z, Lin J, Huang M (2015) Nanoscale 7: 20539-20546.

42. Yoshii M, Murata Y, Nakabayashi Y, Ikeda Y, Fujishima M, Tada H (2016) Colloid Interface Sci 474: 34-40.

43. Pop LC, Sygellou L, Dracopoulos V, Andrikopoulos KS, Sfaelou S, Lianos P (2014) Catal Today 252: 157-161.

44. Legrand-Buscema C, Malibert C, Bach S (2022) Thin Solid Films 418: 79-84.

45. Peng YH, Huang GF, Huang WQ (2012) Visible-light absorption and photocatalytic activity of Cr-doped TiO_2 nanocrystal films, Advanced Power Technology 23: 8-12.

46. Li C, Hsieh JH, Cheng JC, Huang CC (2014) Optical and photoelectrochemical studies on Ag2O/TiO2 double-layer thin films. Thin Solid Films 570: 436-444.

47. Wang W, Li F, Zhang D, Leung YC, Li G (2016) Applied Surface Science. 362: 490-497.

48. Zhao Q (2015) Applied Surface Science 344: 107.

49. Xu J, Yang X, Wang HK, Chen X, Luan CY, et al. (2011) Nano Letters 11: 4138.

50. Robel I, Kuno M, Kamat PV (2007) J Am Chem Soc 129: 4136-4137.

51. Haonan Ge, Feiyan Xu, Bei Cheng, Jiaguo Yu, Wingkei Ho (2019) Chem Cat Chem 11: 6301-6309

52. Van de Walle CG and Neugebauer J (2003) Nature 423: 626-628.

53. Tung Ha Thanh, Dat Huynh Thanh,Vinh Quang Lam (2014) Advances in Opto Electronics 12: 9.

54. Joudi F, Chakhari W, Ouertani R, Ben Naceur J, Chtourou R (2018) Journal of Materials Science: Materials in Electronics.

55. Oliva FY, Avalle LB, Santos E, Cámara OR (2002) Journal of Photochemistry and Photobiology, A: Chemistry 146: 175-188.

56. Allam NK, Shankar K, Grimes CA (2008) Journal of Materials Chemistry. 18: 2341- 2348.

57. Chakhari W, Ben Naceur J, Ben Taieb S, Ben Assaker I, Chtourou R (2017) Journal of Alloys and Compounds 708: 862-870.

58. Seung Wook Shin, Jeong Yong Lee, Kwang-Soon Ahn, Soon Hyung Kang, Jin Hyeok, Kim (2015) J Phys Chem 119: 13375-13383.

59. Vinodgopal K, Hotchandani S, Kamat PV (1993) Journal of Physical Chemistry 97: 9040-9044.

60. Parkinson B (1984) Chem Res 17: 431-437.

61. Dai Y, Sun Y (2014) J Mater Chem A 2: 1060-1067.

62. Boeningo M (1994) Gov. Printing DNHS (NI0ST-I) publication N°66, Washington DC, U.S, 80-119.

63. Prabhakar Y, Gupta A, Kaushik A (2019) Process saf. Environ Protect. 131: 116-126.

64. Chen Z, Jin X, Chen Z, Megharaj M, NaiduR () J. Colloid Interface Sci. 361 (2011) 601-663.

65. Chi H, Tang W (2013) Mod Res Catal 2: 19-24.